

Nonlinear Finite Element Analysis of Reinforced Concrete Slab Strengthened with Shear Bolts

*Khalil Belakhdar*¹⁾

¹⁾ Postgraduate Student Researcher, Department of Civil Engineering, Moulay Tahar University Center, Saida, Algeria, be.khalil@gmail.com

ABSTRACT

This paper presents an implementation of a rational three-dimensional nonlinear finite element model for evaluating the behavior of reinforced concrete slabs strengthened with shear bolts under transverse load. The concrete was idealized by using eight-nodded brick elements. While both flexural reinforcement and the shear bolts were modeled as truss elements, a perfected bond between brick elements and truss elements was assumed. The nonlinear behavior of concrete in compression is simulated by an elasto-plastic work-hardening model, and in tension a suitable post-cracking model based on tension stiffening and shear retention models are employed. The steel was simulated using an elastic-full plastic model. The validity of the theoretical formulations and the program used was verified through comparison with available experimental data, and the agreement has proven to be good. A parametric study has been also carried out to investigate the influence of the shear bolts' diameter and number of bolts' rows around the column-slab connection, on the ductility and ultimate load capacity of slabs.

KEYWORDS: Reinforced concrete plates, Nonlinear FE analysis of RC slabs, Shear capacity of concrete slabs, Shear bolts, Punching shear, Slabs strengthening.

INTRODUCTION

Reinforced concrete slabs are one of the important elements in most structural systems; they are relatively thin structural elements, whose main function is to transmit the vertical loading to their supports. Flat plates or beamless slabs have no beams, column capitals or drop panels, which make formwork very simple and widely used, but the great disadvantage of flat plates or slabs supported by columns is that they are highly susceptible to punching shear failure under concentrated loads, compared with slabs supported by beams or walls.

In order to ensure the serviceability and strength

requirements of such slabs, it is necessary to accurately predict their overall deformational characteristics throughout the range of their elastic and inelastic response as well as their strength at ultimate collapse. Although the need for experimental research to provide the basis for design equations continues, the development of powerful and reliable analytical techniques, such as finite element method, can, however, reduce the time and cost of otherwise expensive experimental tests, and may better simulate the loading and support conditions of the actual structure. Accurate results of finite element analysis, however, require adequate modeling of the actual behavior of reinforced concrete materials including nonlinearity. Reinforced concrete exhibits nonlinearity because of cracking, inelastic material behavior, stiffening and softening phenomena, complexity of bond

between reinforcement and concrete and other factors (Chen and Saleeb, 1982). The derivation and implementation of various analytical finite element and material models to investigate the structural and deformational behavior of reinforced concrete slabs and materials modeling have been the subject of many researches. However, the majority of these researches studied different behavioral aspects of reinforced concrete slabs (Vidoso et al., 1988; Marzouk and Chen, 1993; Marzouk and Jiang, 1996; Jiang and Mirza, 1997; Reitman and Yankelevsky, 1997; Polak, 1998, 2005; Staller, 2000; Salim and Sebastian, 2002; Vainiunas et al., 2004; Murray et al., 2005; Deaton, 2005; Smadi and Belakhdar, 2007) and others.

On the other hand, the punching shear reinforcement has been studied by various researchers. Many experimental investigations are carried out on such reinforcements which are sometimes supported by theoretical investigations (Hawkins, 1974; Dilger and Ghali, 1981; Mokhtar, Ghali and Dilger, 1985; Elgabry and Ghali, 1990; Lim and Rangan, 1995; Marzouk and Jiang, 1996; El-Salakawy, Polak and Soliman, 2000; Alaa et al., 2000; Adetifa and Polak, 2005). These investigations confirm that shear reinforcement in slabs is effective in increasing punching shear, ductility and, therefore, increasing rotation capacities of the connection if the proper amount of reinforcement, placement and spacing and anchorage conditions are satisfied.

The present work is a numerical study which is conducted to predict the behavior up to ultimate conditions of slab-column connections strengthened with shear bolts under transverse loads. The performance of slabs is evaluated in terms of load-deflection characteristics. The validity and calibration of the theoretical formulations and the program used is judged through comparison of analytical results with available experimental data. Finally, a parametric study is carried out to investigate the influence of bolts' properties on the behavior of slabs.

FINITE ELEMENT FORMULATION

Modeling of concrete material in compression

The behavior of concrete in compression is simulated

by an elasto-plastic work hardening model up to the onset of crushing. Generally, according to the incremental theory of plasticity, the total strain increment is usually assumed to be the sum of elastic strain and plastic strain. The formulation of the constitutive relations in the work-hardening plastic model is based on three fundamental assumptions (Chen and Saleeb, 1982; Kwak and Filippou, 1990; Al-Shaarbaf, 1990; Crisfield, 1994): The shape of the initial yield surface (failure criteria), the evolution of the hardening rule and formulation of an appropriate flow rule. However, the plasticity model and its constituents, and the modeling of concrete under triaxial state of stress, will be discussed in terms of the following elements: 1) Uniaxial stress-strain relationship, 2) Failure criterion, 3) Hardening rule, 4) Flow rule and 5) Crushing condition.

Uniaxial stress-strain relationship

Frequently, the widely used stress-strain relationship of concrete up to the peak stress is given as a parabolic relationship as follows (Foster et al., 1996; Pang and Hsu, 1996; Bahn and Hsu, 2000; Wang and Hsu, 2001):

$$\sigma = f_c' \left[\frac{2\varepsilon}{\varepsilon_0} - \left(\frac{\varepsilon}{\varepsilon_0} \right)^2 \right] \quad (1)$$

where ε_0 is the strain at peak stress f_c' given by

$$\varepsilon_0 = 2 \cdot \frac{f_c'}{E_c} \quad (2)$$

In the present study, to accurately simulate the uniaxial stress-strain curve of both normal and high strength concrete, the equivalent uniaxial stress-strain relationship used is composed of two parts. The first is linear and the other is parabolic. The linear part is given by:

$$\sigma = E_c \cdot \varepsilon_e \quad (3)$$

where ε_e is the elastic strain and σ is the corresponding stress.

The parabolic part alone has the same form as Equation (1). This part starts beyond the limit of elasticity which is limited at $(\zeta.f_c)$, where ζ is the elastic limit coefficient ($0 \leq \zeta \leq 1$) used to indicate the limit of

elastic part and initiation of plastic deformation. Therefore, typical stress-strain relationship of concrete is obtained by using the assembled model shown in Fig. 1.

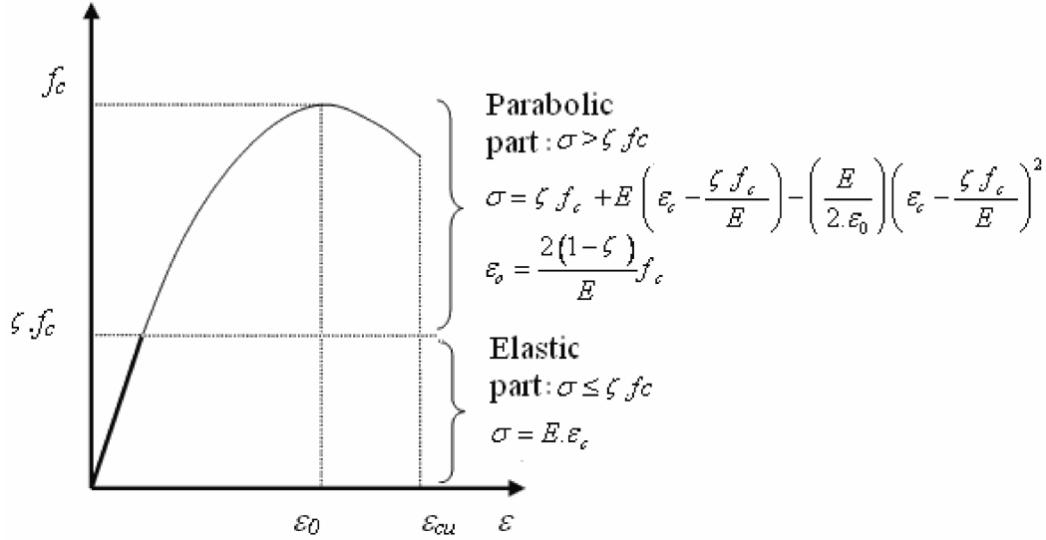


Fig. (1): Stress-strain relationship for concrete.

Thus, the total equivalent uniaxial stress-strain curve can be expressed as follows:

For $\sigma \leq \zeta.f_c$

$$\sigma = E_c . \varepsilon_c \tag{4}$$

For $\sigma \geq \zeta.f_c$

$$\sigma = \zeta.f_c + E_c \left(\varepsilon_c - \frac{\zeta.f_c}{E_c} \right) - \left(\frac{E_c}{2.\varepsilon_0} \right) \left(\varepsilon_c - \frac{\zeta.f_c}{E_c} \right)^2 \tag{5}$$

where ε_c is the total strain and ε_0 is the total strain at peak stress which can be calculated by:

$$\varepsilon_0 = \frac{2(1-\zeta)}{E_c} f_c \tag{6}$$

In the current study, the elastic limit coefficient is taken to be $\zeta=0.3$.

In the presence of orthogonal cracks which are caused

by shear or transverse tensile stresses, concrete exhibits lower compressive strength and stiffness than in the uniaxially compressed state. Such degradation or softening in compressive strength of concrete is taken into consideration in the present study by multiplying the uniaxial compressive concrete stress defined in Equations (4) and (5) by a softening factor λ , as shown in Fig. 2. Among various compression reduction models available in literature, the model suggested by Vecchio et al. (1994) is implemented in the present finite element formulation. The model can be expressed as:

$$\lambda = \frac{1}{1 + K_c . K_f} \tag{7}$$

where K_c represents the effect of the transverse cracking and straining, K_f represents the dependence on the strength of the concrete (f_c), and K_c and K_f are given by:

$$K_c = 0.27 \left(\frac{\varepsilon_r}{\varepsilon_0} - 0.37 \right) \tag{8}$$

$$K_f = 2.55 - 0.2629\sqrt{f_c'} \leq 1.11 \quad (9)$$

where ε_r is the tensile strain normal to the cracked plane given by:

For cracked sampling point in the principal direction (⊙)

$$\varepsilon_r = \varepsilon_1 \quad (10)$$

For doubly cracked sampling point in both directions (⊙) and (⊚)

$$\varepsilon_r = (\varepsilon_1^2 + \varepsilon_2^2)^{\frac{1}{2}} \quad (11)$$

Where ε_1 is the transverse tensile strain in the principal direction (⊙) normal to the cracked plane, ε_2 is the tensile strain in the second direction (⊚) normal to the second crack plane.

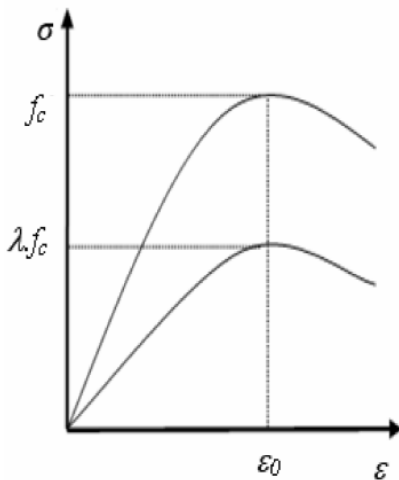


Fig. (2): Compression reduction of transversely cracked concrete.

Failure criterion

Under triaxial state of stress, the failure criterion for concrete is generally assumed to be dependent on three stress invariants. However, the failure criterion used in this study is dependent on two stress invariants and has proved to be adequate for most practical situations and has been successfully used by many investigators for analyzing reinforced concrete plate and shells (Figueiras and Owen, 1984; Cervera and Hinton, 1986; Naji, 1989; Al-Shaarbaf, 1990) which can be expressed as:

$$f(\sigma) = f(I_1, J_2) = \sqrt{\alpha I_1 + 3\beta J_2} - \sigma_0 = 0 \quad (12)$$

where:

I_1 is the first stress invariant;

J_2 is the second deviatoric stress invariant;

σ_0 is the equivalent effective stress at the onset of plastic deformation,

$$\alpha = \sigma_0(\beta - 1) \quad (13)$$

$$\beta = \frac{1 - 2.\gamma}{\gamma^2 - 2.\gamma} \quad (14)$$

where γ is a constant to be determined from the equal biaxial compression state, which is given by:

$$\sigma_x = \sigma_y = -\gamma\sigma_0 \quad (15)$$

However, the constant was found by Hussein and Marzouk (2000) to have values of 19, 14 and 9% for 42.7, 73.7 and 96.5 MPa, respectively; thus in the present study, the value of $\gamma=19$ is adopted.

The hardening rule and flow rule

An isotropic hardening rule is adopted in the present study which implies a uniform expansion of the initial yield surface without translation as plastic deformation increases. The required incremental stress-strain relationship may be obtained by differentiation of equivalent stress-strain relationship with respect to the plastic strain. This operation leads to the slope of the tangent of effective stress-plastic strain curve which represents the hardening coefficient, which is needed in the formulation of the incremental stress-strain relationship. In order to calculate the plastic strain increment for a given stress increment, a flow rule must be defined. The associated flow rule has been widely used to concrete application by many researchers for reason of simplification (Al-Shaarbaf, 1990; Marzouk and Chen, 1993), and it was adopted in the present study.

The crushing condition

The experimental tests of concrete under multiaxial loading indicate that the crushing is a strain related

phenomenon (Chen and Saleeb, 1982), so concrete is considered to crush when the strain reaches a specified ultimate value, after that the current stresses drop suddenly to zero and the concrete is assumed to lose completely its resistance against further deformation. Hence, the crushing criterion is directly obtained by using the same form of yield criterion but in terms of strains, as follow:

$$C.I_1 + \sqrt{(C.I_1)^2 + 3.\beta.J_2} = \epsilon_{cu} \tag{16}$$

where:

I_1 : The first strain invariant;

J_2 : The second deviatoric strain;

ϵ_{cu} : The ultimate concrete strain that can be obtained from the uniaxial compression test.

If Eqn. (16) is satisfied or the strain is greater than the specified ϵ_{cu} , in this case the concrete is assumed to be crushed and the structure is ruptured, therefore the analysis stopped. Frequently, the ultimate concrete crushing strain ϵ_{cu} is estimated to be in the range of 0.0030 as suggested by ACI-318-02 and NZS-95 codes to 0.0035 as given by BS8110 and CSA-94 codes. Based on experimental tests of singly reinforced concrete beams or eccentrically loaded columns without lateral confinement steel, the ultimate strain measured at the extreme compression face at failure was found to decrease as the ultimate compressive strength of concrete increases as shown in Fig. 3 (ACI Committee 363R-92, 1997). Consequently, the value of the crushing strain ϵ_{cu} is taken as 0.0035.

Modeling of concrete materials in tension

When tensile stress exceeds a limiting value, a crack is assumed to form in the plane perpendicular to the direction of that stress and concrete behaves no longer isotropic, and, therefore, the normal stiffness is reduced through tension-stiffening concept. Once concrete has cracked, fixed smeared cracking model is used in the current study to model the crack. The gradual release of tensile stresses normal to the cracked plane is represented by bilinear average stress-strain curves to simulate the tension stiffening behavior. Noting that the majority of models used in numerical analysis and implemented in

finite element formulation are idealized as linear or bilinear curves (Sam and Lyer, 1995; Staller, 2000; Polak, 2005) as follows (Fig. 4):

For $\epsilon_{cr} \leq \epsilon_n \leq \alpha_1 \epsilon_{cr}$

$$\sigma_n = \alpha_2 \sigma_{cr} \left(\frac{\alpha_1 - \frac{\epsilon_n}{\epsilon_{cr}}}{\alpha_1 - 1} \right) \tag{17}$$

For $\epsilon_n > \alpha_1 \epsilon_{cr}$

$$\sigma_n = 0 \tag{18}$$

where:

σ_n , ϵ_n are the stress and strain normal to the cracked plane;

σ_{cr} , ϵ_{cr} are the cracking stress and its corresponding cracking strain;

α_1 is the parameter of tension stiffening which represents the rate of stress release as the crack widens;

α_2 is the parameter of tension stiffening which represents the sudden loss of stress at the instant of cracking.

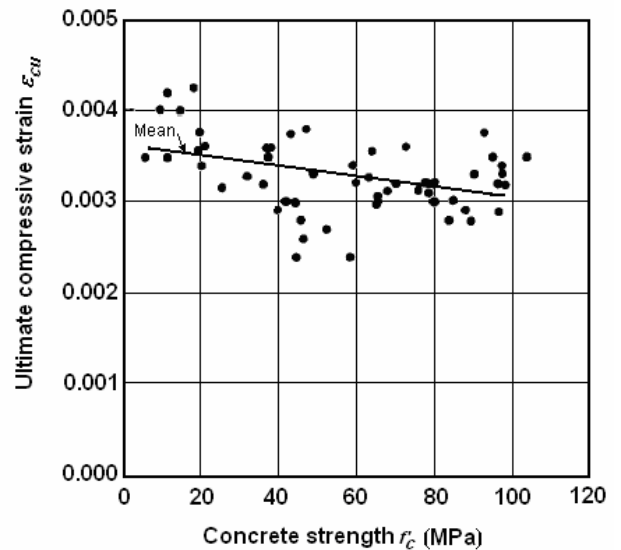


Fig. (3): Ultimate compressive strain versus compressive strength of concrete (ACI Committee 363R-92, 1997).

The shear stiffness is also reduced when cracking occurs, because it retains the two major mechanisms by which shear is transferred across the crack (the aggregate interlock of the rough crack surfaces and dowel action of the reinforcing bars crossing the crack planes). A bilinear shear retention model is used as shown in Fig. 5. This model can be represented as follows:

For $\epsilon_n \leq \epsilon_{cr}$

$$\beta = 1.0 \tag{19}$$

For $\epsilon_{cr} \leq \epsilon_n \leq \gamma_1 \epsilon_{cr}$

$$\beta = \frac{\gamma_2 - \gamma_3}{\gamma_1 - 1} \left[\gamma_1 - \frac{\epsilon_n}{\epsilon_{cr}} \right] + \gamma_3 \tag{20}$$

For $\epsilon_n > \gamma_1 \epsilon_{cr}$

$$\beta = \gamma_3 \tag{21}$$

where $\gamma_1, \gamma_2, \gamma_3$ are shear retention parameters.
 γ_1 represents the rate of decay of shear stiffness as the crack widens;
 γ_2 is the sudden loss in shear stiffness at the instant of cracking;
 γ_3 is the residual shear stiffness due to the dowel action.

The material parameters used in the analysis are as follow:

Tension stiffening: $\alpha_1 = 5, \alpha_2 = 0.6$;
 Shear retention: $\gamma_1 = 10, \gamma_2 = 0.5, \gamma_3 = 0.04$.

Besides, at onset of cracking Poisson's ratio (ν_c) is set to zero.

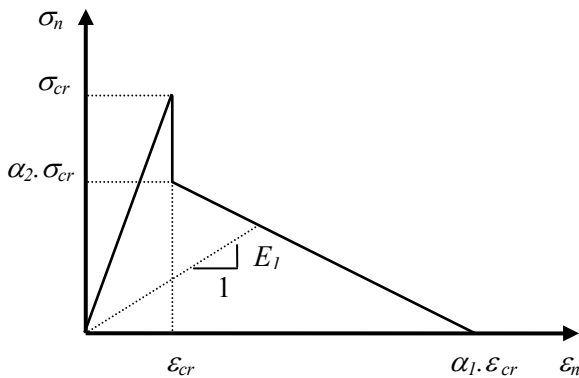


Fig. (4): Bilinear average tensile stress-strain of concrete.

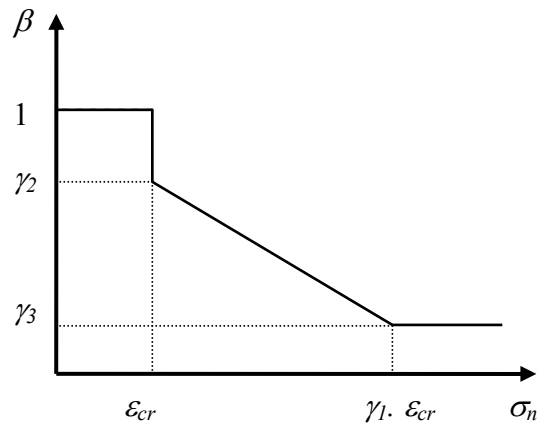


Fig. (5): Bilinear shear retention model.

Material modeling of reinforcement

In contrast to concrete, the material modeling of steel is rather simple. Frequently, the steel is modeled using linear elastic-full plastic model, as shown in Fig. 6.

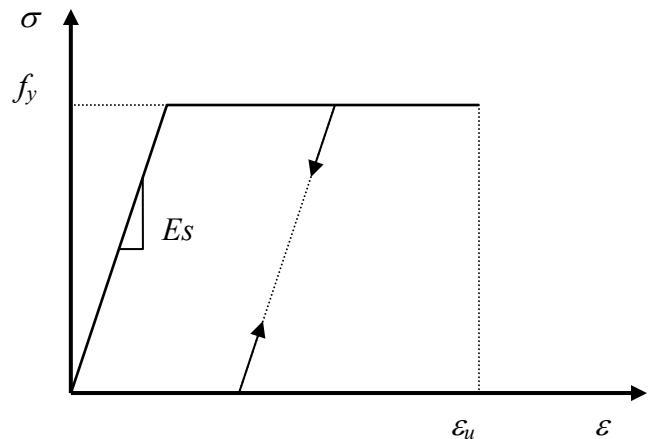


Fig. (6): Modeling of steel reinforcing bars.

FINITE ELEMENT IDEALIZATION

The concrete is represented by using 8-noded brick element. The reinforcing bars and the shear bolts are modeled as one dimensional element subjected to axial force only, and perfect bond is assumed to occur between the two materials, as shown in Fig. 7.

The non-linear equations of equilibrium have been solved using the incremental-iterative technique based on

the modified Newton-Raphson method. The convergence of the solution was controlled by a load convergence criterion.

By taking advantage of symmetry, a segment representing one quarter of the slabs has been considered

in the finite element analysis, as shown in Fig. 7. A fine mesh size has been used which consists of 2048 brick elements, noting that the same mesh characteristics were kept throughout this study.

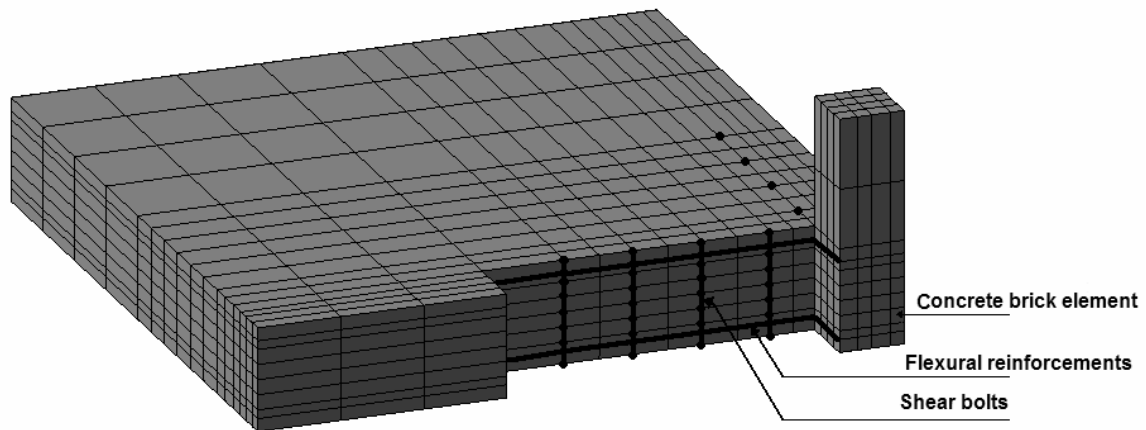


Fig. (7): Finite element mesh.

VALIDATION OF THE ANALYTICAL RESULTS

Description of selected experimental slabs

Four simply supported square slabs strengthened against punching shear using shear bolts were used to validate and corroborate the predicted analytical results. The selected experimental slabs were carried out by Adetifa and Polak (2005). The slabs have the same dimensions of 1800 x 1800 x 120 mm, where the simple supports were applied at the in-plane distances of 1500 x 1500 mm as shown in Fig. 8. All slabs have same amount and placement of orthogonal longitudinal reinforcement. 9.5 mm-diameter shear bolts were arranged in concentric rows parallel to the perimeter of the column. Each concentric row consisted of eight bolts two parallel to each face of the square column. The first row was placed at approximately 50mm from the face of the column and subsequent rows were spaced at 80mm as shown in Fig. 9. Additional information on material and geometric properties of these slabs are fully listed in Table 1. The following material properties are assumed in the FE analysis: $E_s=200.000\text{MPa}$, $E_c = 4700 \cdot \sqrt{f_c}$ and $\nu_c=0.20$.

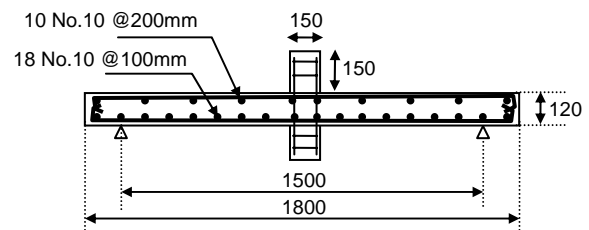


Fig. (8): Geometrical dimensions of selected slabs.

Results of the analysis

The results of the present nonlinear finite element analysis of the investigated slabs in terms of ultimate load are compared against the experimental measurements and listed in Table 2. Fig. 10 shows load-deflection curves of selected slabs of the present finite element analysis and experimental results. Table 2 indicates that the predicted to experimental ultimate load ranges from 0.986 to 1.083 with a standard deviation of 0.042. According to Fig. 10, it can be observed that the present finite element model performs satisfactorily and it predicts accurately the real behavior of slabs.

Table 1: Slabs’ geometric and material properties.

Slab	Compressive strength (MPa)	Tensile concrete strength, (MPa)	Yield strength of flexural reinforcement, (MPa)	No. of rows of shear bolts	Yield strength of shear bolts, (MPa)
SB1	44	2.2	455	-	-
SB2	41	2.1	455	2	381
SB3	41	2.1	455	3	381
SB4	41	2.1	455	4	381

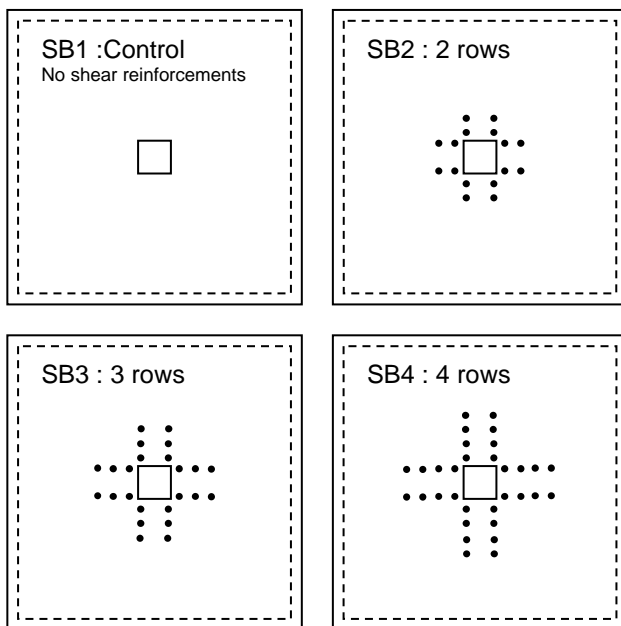


Fig. (9): Locations of shear bolts.

PARAMETRIC STUDIES

Effect of the shear bolts’ diameter

A numerical analysis was carried out on the slab SB4 using two values of bolts’ diameter (9.5mm and 12mm), the results of which are shown in Fig. 11. It can be seen that prior to yielding point the bolts’ diameter does not

influence the load-deflection characteristics. However, after yielding, the load deflection curve becomes quite stiffer. Also both the ultimate load and deflection increase as the bolts’ diameter increases. From the load deflection curve, it can be observed that the bolts’ diameter alters the mode of failure where the slab behaviour becomes ductile in case of 12mm diameter.

Effect of the number of rows

To study the effect of the number of rows on slab behavior, the selected slabs were analyzed keeping the same number of rows (0, 2, 3, 4 rows). The results obtained in terms of slab load-deflection relationships are presented in Fig. 12. From this figure, it can be seen that adding bolts on slabs has a significant effect on improving the load carrying capacity of slabs, and it increases the ultimate deflection. On the other hand, as the number of rows increases, the slab behavior becomes stiffer but more ductile just after cracking.

Fig. 13 and Fig. 14 clarify the effect of both diameter of shear bolts and the number of bolts’ rows around the column on the predicted ultimate load and ultimate deflection. These figures show an improvement of slab strength with the increase in the number of shear bolts’ rows. Furthermore, the ultimate deflection using 4 rows is about 3 times greater than the same slab without shear bolts; hence, using shear bolts has a considerable effect on improving the ductility of column-slab connections.

Table 2: Comparison of the predicted and experimental results.

Slab	First yielding load		Ultimate load P_u (kN)			Ultimate central deflection D_u (mm)		
	Exp.	FEA	Exp.	FEA	FEA / Exp	Exp.	FEA	FEA / Exp
SB1	240	245	253	260.50	1.03	11.9	14.32	1.20
SB2	224	230	364	359.00	0.99	27.6	32.61	1.18
SB3	260	233	372	375.20	1.01	31.0	34.70	1.12
SB4	240	235	360	390.00	1.08	38.9	37.50	0.96
			Ave.	1.03		Ave.	1.12	
			St.Dev.	0.04		St.Dev.	0.11	

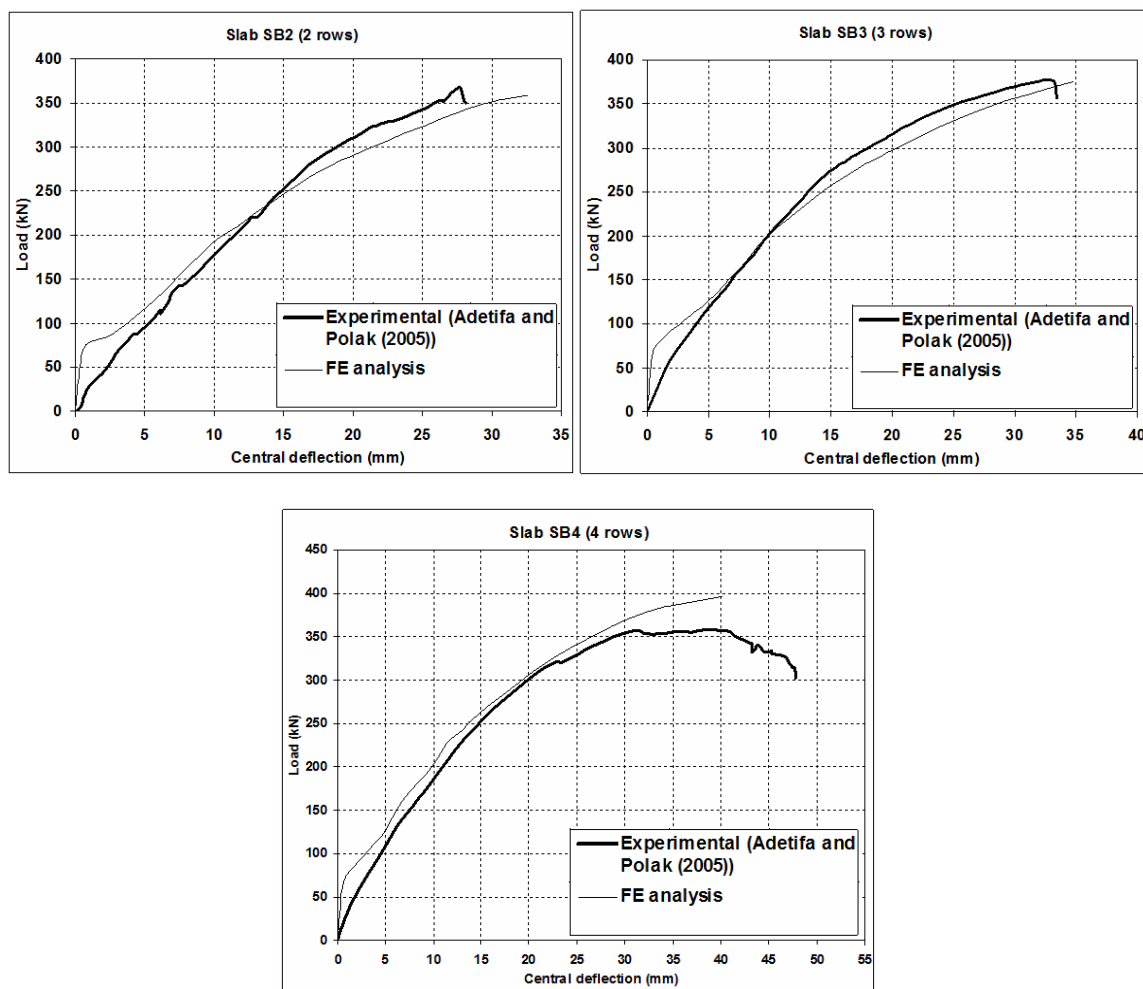


Fig. (10): Comparison of predicted and experimental load-deflection curves.

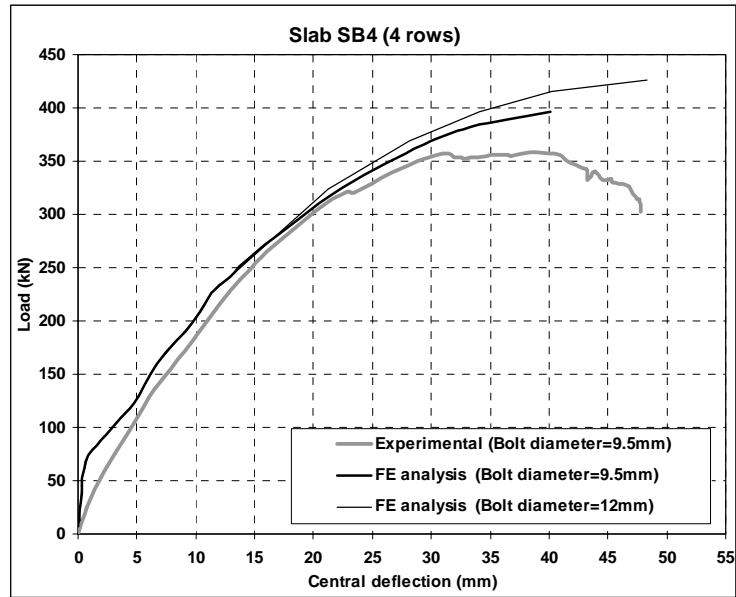


Fig. (11): Effect of the shear bolts' diameter.

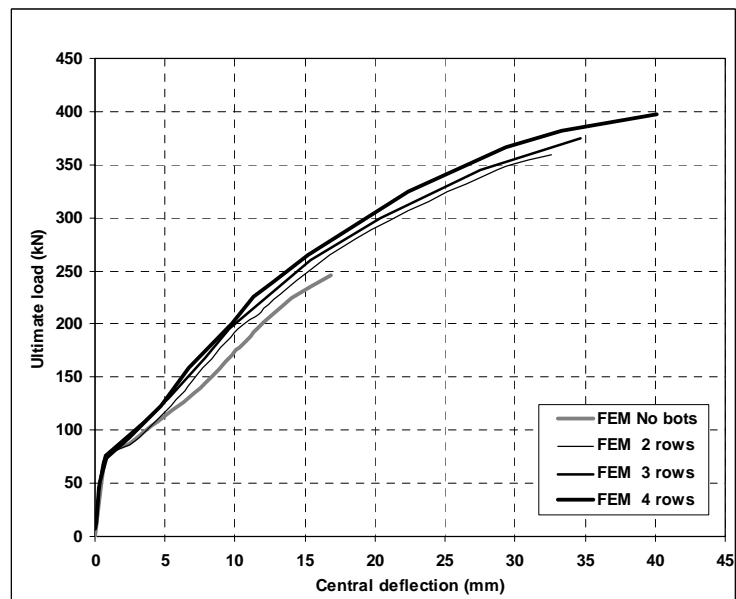


Fig. (12): Effect of the number of rows.

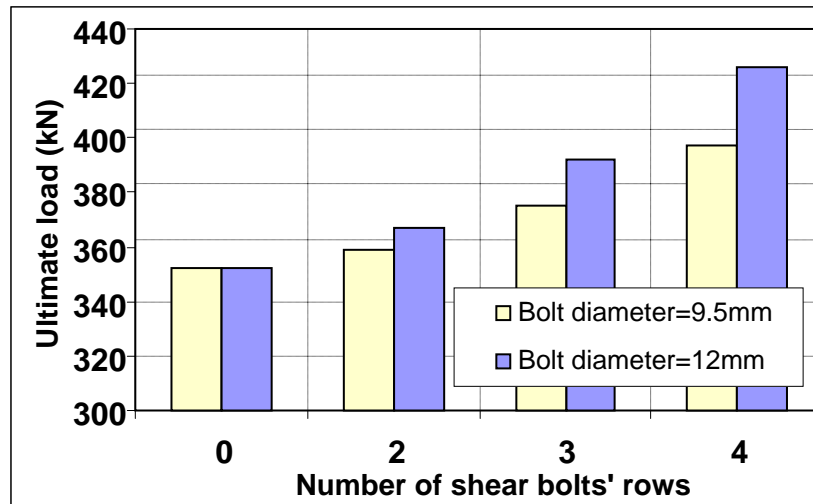


Fig. (13): Effect of the number of shear bolts' rows and bolts' diameter on the ultimate load of slab.

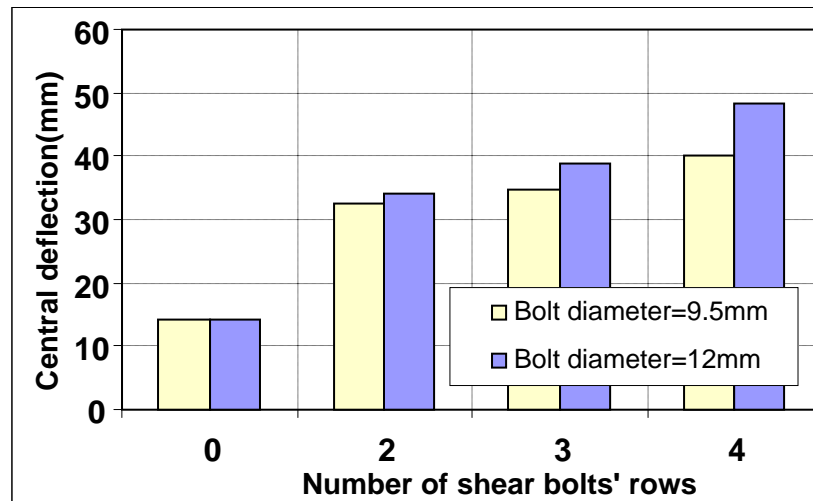


Fig. (14): Effect of the number of shear bolts' rows and bolts' diameter on the central deflection of slab.

CONCLUSIONS

A computer program suitable for nonlinear analysis of three dimensional reinforced concrete members under monotonic increasing loads has been developed to simulate the behavior of slabs strengthened with shear bolts. The concrete is represented by using 8-noded brick elements, while the reinforcing bars and the shear bolts are modeled as one dimensional element. The nonlinear

behavior of concrete in compression is simulated by an elasto-plastic work-hardening model up to the onset of crushing. A fixed smeared crack model has been used with tension-stiffening model. A shear retention model that modifies the shear stiffness and a softening model that reduces the concrete compressive strength due to cracking are also implemented.

Various aspects of slab behavior were predicted using

proper material models and NLFE program and compared with available experimental data. The comparison was judged to be good, and the analytical formulations were capable of accurately predicting the total response and capacity of the concrete slabs. An analytical parametric-study was carried out to investigate the effect of shear bolts' parameters on the slab's behaviour. The following conclusions may be drawn from the present study:

1- Nonlinear finite element method based on advanced 3D models is a powerful and relatively economical tool which can be effectively used to simulate the true behavior of reinforced concrete slabs even

under complex conditions.

- 2- The choice of adequate material models for numerical simulation is the most important aspect in finite element modeling of concrete structures.
- 3- Using shear bolts to strengthen column-slab connection against punching shear phenomenon is simple and easy to install, and it effectively improves the capacity of the slab.
- 4- The use of shear bolts increases the maximum deflection and consequently increases ductility, which improves the column-slab connection capacity.

REFERENCES

- ACI Committee 363R-92. 1997. State-of-the-Art Report on High-Strength Concrete, (*ACI 363R-92*): 55.
- ACI Committee 435. 1991. States of the Art Report on Control of Two Way Slab Deflections, *ACI Structural Journal*, 88 (4): 501-514.
- Al-Shaarbaf, I. 1990. Three-Dimensional Non-Linear Finite Element Analysis of Reinforced Concrete Beams in Torsion, *PhD Thesis*, University of Bradford.
- Attard, M.M. and Stewart, M.G. 1998. A Two Parameter Stress Block for High-Strength Concrete, *ACI Structural Journal*, 95 (3): 305-317.
- Bahn, B.Y. and Hsu, T.T.C. 2000. Cyclically and Biaxially Loaded Reinforced Concrete Slender Columns, *ACI Structural Journal*, 97 (3): 444-454.
- Belakhdar, K.A. 2006. Three Dimensional Nonlinear Finite Element Analysis of High Strength Reinforced Concrete Slabs, *M.Sc Thesis*, Faculty of Graduate Studies, Jordan University of Science and Technology, Irbid, Jordan, 188.
- Cervera, M. and Hinton, E. 1986. Nonlinear Analysis of Reinforced Concrete Plates and Shells using a Three Dimensional Modeling of Reinforced Concrete Structures, Pineridge Press, Swansea, UK, 327-370.
- Chen, W.F. and Saleeb, A.F. 1982. Constitutive Equations for Engineering Material, John Wiley and Sons, New York, 1: 580.
- Chung, W. and Ahmed, H. 1994. Model for Shear Critical High Strength Concrete Beams, *ACI Structural Journal*, 91 (1): 31-41.
- Crisfield, M.A. 1994. Nonlinear Finite Element Analysis of Solids and Structures, Department of Aeronautics, Imperial College of Science, Technology and Medicine, London, UK, John Wiley and Sons, 1: 345.
- Dahl, K.K.B. 1992. Uniaxial Stress-Strain Curves for Normal and High Strength Concrete, *ABK Report No.R282*, Department of Structural Engineering, Technical University of Denmark.
- Deaton, J.B. 2005. A Finite Element Approach to Reinforced Concrete Slab Design, *M.Sc Thesis*, School of Civil and Environmental Engineering, Georgia Institute of Technology, 170.
- Fields, K. and Bischoff, P. 2004. Tension Stiffening and Cracking of High-Strength Reinforced Concrete Tension Members, *ACI Structural Journal*, 101 (4): 447-456.
- Figueiras, J.A. and Owen, R.J. 1984. Nonlinear Analysis of Reinforced Concrete Shell Structures, *Proceedings of the International Conference on Computer Aided Analysis and Design of Concrete Structures*, Yugoslavia.
- Foster, S.J., Budiono, B. and Gilbert, R.I. 1996. Rotating Crack Finite Element Model for Reinforced Concrete Structures, *Computer and Structure*, 58 (1): 43-50.
- Hussein, A. and Marzouk, H. 2000. Behavior of High-strength Concrete under Biaxial Stresses, *ACI Material Journal*, 97 (1): 27-36.
- Jiang, J. and Mirza, F. 1997. Nonlinear Analysis of Reinforced Concrete Slabs by Discrete Finite Element

- Approach, *Computer and Structure*, 65 (4):1667-1687.
- Kwak, H.G. and Filippou, F.C. 1990. Finite Element Analysis of Reinforced Concrete Structures under Monotonic Loads, *Structure Engineering Mechanics and Materials*, Report No.USB/SEMM-90/14, Department of Civil Engineering, University of California, Berkely, 120.
- Marzouk, H. and Chen, Z. 1993. Finite Element Analysis of High Strength Concrete Slabs, *ACI Structural Journal*, 90 (5): 505-513.
- Marzouk, H. and Jiang, D. 1996. Finite Element Evaluation of Shear Enhancement of High Strength Concrete Plates, *ACI Structural Journal*, 93 (6), 667-673.
- Murray, K.A., Cleland, D.J. and Gilbert, S. 2005. The Development of Non-linear Numerical Model to Simulate the Behaviour of Reinforced Concrete Flat Slabs in the Vicinity of Edge Columns, *Construct. Bldg. Mater.*, 19: 703-712.
- Naji, J.H. 1989. Non-linear Finite Element Analysis of Reinforced Concrete Panels and Infilled Frames under Monotonic and Cyclic Loading, *PhD Thesis*, University of Bradford.
- Pang, X.B. and Hsu, T.T.C. 1996. Fixed Angle Softened Truss Model for Reinforced Concrete, *ACI Structural Journal*, 93 (2): 197-207.
- Polak, M.A. 2005. Ductility of Reinforced Concrete Flat Slab-column Connections, *Computer Aided Civil Infrastructure Engineering*, 20: 184-193.
- Polak, M.A. 1998. Modelling Punching Shear of Reinforced Concrete Slabs using Layered Finite Elements, *ACI Structural Journal*, 95 (1): 71-80.
- Reitman, M. and Yankelevsky, D. 1997. A New Simplified Model for Nonlinear RC Slabs Analysis, *ACI Structural Journal*, 94 (4): 399-408.
- Salim, W. and Sebastian, W. 2002. Plasticity Model for Predicting Punching Shear Strengths of Reinforced Concrete Slabs, *ACI Structural Journal*, 99 (6): 827-835.
- Sam, C. and Lyer, P.K. 1995. Nonlinear Finite Element Analysis of Reinforced Concrete Four Pile Caps, *Computer and Structure*, 57 (4): 605-622.
- Shanmugam, N.E., Kumar, G. and Thevendram, V. 2002. Finite Element Modeling of Double Skin Composite Slabs, *Finite Elements in Analysis and Design*, 38: 579-599.
- Smadi, M.M. and Belakhdar, K.A. Nonlinear Finite Element Analysis of High Strength Concrete Slabs, *Computers and Concrete*, 4 (3): 187-206.
- Staller, D. 2000. Analytical Studies and Numerical Analysis of Punching Shear Failure in Reinforced Concrete Slabs, *TRITA-BKN Bulletin*, 57: 8.
- Thabet, A. and Haldane, D. 2000. Three-dimensional Simulation of Nonlinear Response of Reinforced Concrete Members Subjected to Impact Loading, *ACI Structural Journal*, 97 (5): 698-702.
- Tomaszewicz, A. 1993. High-strength Concrete, SP2 (*Plates and Shells, Report 2.3, Punching Shear Capacity of Reinforced Concrete Slabs*; Report No. STF70A93082): SINTEF, Trondheim, 36.
- Vainiunas, P., Popovas, V. and Vilnius, A.J. 2004. Nonlinear FEA of RC Floor Slab-to-Column Joint Connection, *Theoretical Foundations of Civil Engineering-XII*, Ed. by W. Szczesninak, OW PW, Warsaw, 12.
- Vecchio, F. and Collins, M. 1986. The Modified Compression Field Theory for Reinforced Concrete Element Subjected to Shear, *ACI Journal*, 83 (2): 219-231.
- Vecchio, F., Collins, M. and Aspiotis, J. 1994. High Strength Concrete Elements Subjected to Shear, *ACI Structural Journal*, 91 (4): 423-433.
- Vidoso, F., Kotsovos, M. and Pavlovic, M. 1988. Symmetrical Punching of Reinforced Concrete Slabs: An Analytical Investigation Based on NFE Modelling, *ACI Structural Journal*, 85 (2): 241-250.
- Wang, T. and Hsu, T.C C. 2001. Nonlinear Finite Element Analysis of Concrete Structures Using New Constitutive Models, *Computer Structure*, 79: 2781-2791.